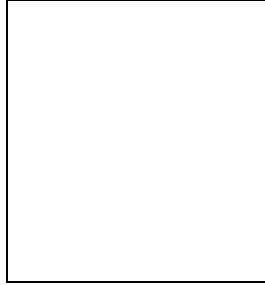


## Electroweak Results from LEP and SLC and Tests of the Standard Model

E. TOURNEFIER

*ISN Grenoble, 53, avenue des Martyrs,  
38026 Grenoble, France*



An update of the electroweak measurements at LEP and SLC is presented. These measurements are used to perform precise tests of the Standard Model. A constraint on the Standard Model Higgs mass is obtained when the direct measurements of  $m_{\text{top}}$  and  $M_W$  are included in the fit. A combination with the direct Higgs search is also shown.

### 1 Introduction

The precise electroweak measurements which have been performed at LEP and at SLC allow to make precise tests of the Standard Model and to constrain the Higgs mass.

At the  $Z$  resonance the cross sections and the asymmetries of the process  $e^+e^- \rightarrow Z, \gamma \rightarrow f\bar{f}$  are sensitive to  $m_t^2$ ,  $\alpha_s$  and  $\text{Log}(M_H)$  through radiative corrections. The electroweak corrections to  $e^+e^- \rightarrow f\bar{f}$  lead to the running of the electromagnetic coupling constant  $\alpha_{\text{QED}}$  and corrections to the coupling constants of the  $Z$  to fermions. These corrections are absorbed in the definition of the effective electroweak mixing angle  $\sin^2\theta_{\text{eff}}^{\text{lept}}$  and of  $\bar{\rho}$ :  $\sin^2\theta_{\text{eff}}^{\text{lept}} = (1 + \Delta\kappa) \sin^2\theta_W$ ,  $\bar{\rho} = 1 + \Delta\rho$  where  $\sin^2\theta_W = 1 - M_W^2/M_Z^2$  and  $\rho = M_W^2/(M_Z^2 \cos^2\theta_W) = 1$ .

The measurement of the asymmetries determines the values of  $A_l = \frac{2g_V/g_A}{1+(g_V/g_A)^2}$  which are converted into the effective electroweak mixing angle  $\sin^2\theta_{\text{eff}}^{\text{lept}} = \frac{1}{4}(1 - \frac{g_V}{g_A})$ , one of the most sensitive variables to the Higgs mass. On the other hand the measurement of the cross sections allows the determination of  $\bar{\rho}$  which is more sensitive to the top mass.

The  $W$  mass also includes radiative corrections:  $M_W^2 = \frac{\pi\alpha}{\sqrt{2}\sin^2\theta_W G_f}(1+\Delta r)$  with  $\Delta r = \Delta\alpha + \Delta r_W$ . The values of these corrections,  $\Delta\rho$ ,  $\Delta\kappa$  and  $\Delta r_W$  depend quadratically on  $m_{\text{top}}$  and only logarithmically on  $M_H$ , leading to a much weaker constraint on  $M_H$  than on  $m_{\text{top}}$ .

## 2 The electroweak measurements

In this section the status of the main electroweak measurements used in the fit to the Standard Model is given as well as the most significant new inputs.

### 2.1 Status of the measurements

The main electroweak measurements used in the fit are

- LEP1 and SLC electroweak measurements at the Z resonance:  
The Z lineshape parameters from LEP1, the Z mass  $M_Z$ , the Z width  $\Gamma_Z$ , the hadronic pole cross section  $\sigma_{\text{had}}^0$ ,  $R_l = \Gamma_{\text{hadrons}}/\Gamma_l$  and the forward-backward leptonic asymmetries  $A_{\text{FB}}^{0,l} = \frac{3}{4}\mathcal{A}_e\mathcal{A}_l$  are final<sup>1</sup>.  
The  $\tau$  polarisation,  $\mathcal{P}_\tau$  at LEP1 is also final.  $\mathcal{A}_e$  and  $\mathcal{A}_\tau$  are derived from this measurement. The measurement of the left-right asymmetry  $A_{\text{LR}}^0 = \mathcal{A}_e$  and of the leptonic left-right forward-backward asymmetries  $A_{\text{FB}}^{\text{LR}}$  at SLC are final.  
LEP1 and SLC also provide measurements of the Z decay fractions into  $b$  and  $c$  quarks  $R_b^0$ ,  $R_c^0$ . The  $b\bar{b}$  and  $c\bar{c}$  asymmetries  $A_{\text{FB}}^{0,b\bar{b}}$ ,  $A_{\text{FB}}^{0,c\bar{c}}$  as well as the quark charge asymmetry  $\langle Q_{\text{FB}} \rangle$  are determined at LEP1 while  $A_b$  and  $A_c$  are measured at SLC. ALEPH and DELPHI have significantly improved their  $A_{\text{FB}}^{0,b\bar{b}}$  measurement<sup>2,3</sup> (see section 2.2). SLD has updated its heavy flavour results<sup>4</sup>.
- LEP2 and  $p\bar{p}$  colliders measurements of the W mass:  $M_W$  from LEP includes the data taken in 2000 for ALEPH and L3<sup>5</sup>, this will be discussed in section 2.2.
- The top mass measurement from CDF and D0 which is final.
- The determination of  $\sin^2\theta_W$  by NuTeV.
- Another important input used in the fit is the QED coupling constant at the Z mass  $\alpha_{\text{QED}}(M_Z^2)$ . New low energy  $e^+e^-$  data taken by BES<sup>6</sup> at BEPC have been used to obtain a new experimental determination of  $\alpha_{\text{QED}}(M_Z^2)$ <sup>7</sup> (see section 2.2).

Details and references to these measurements can be found in Reference<sup>8,9</sup>.

### 2.2 The most significant new inputs

$A_{\text{FB}}^{0,b\bar{b}}$

A new analysis<sup>3</sup> has been used by DELPHI leading to an improved determination of  $A_{\text{FB}}^{b\bar{b}}$ . This analysis is based on a neural network to tag the b-charge using the full available charge information from vertex charge, jet charge and from identified leptons and hadrons. A double tag method is used to calibrate this neural network tag on the data leading to a reduced systematic uncertainty. Note that this measurement is correlated with the measurement obtained with the *jet-charge* and with the *leptons* measurements shown in Figure 1. The new value (referred to as DELPHI NN on Figure 1) is

$$A_{\text{FB}}^{b\bar{b}}(\sqrt{s} \simeq M_Z) = 0.0931 \pm 0.0034 \pm 0.0015 \quad (1)$$

ALEPH has improved its  $A_{\text{FB}}^{b\bar{b}}$  jet-charge measurement<sup>2</sup>. A neural network has been used to tag b-events leading to a 30% increase in statistics while keeping the same purity. The jet-charge estimator has been improved, reducing the mistag rate by 10%. The systematic uncertainties are better controlled by the use of double-tag methods for both flavour and charge tags. With

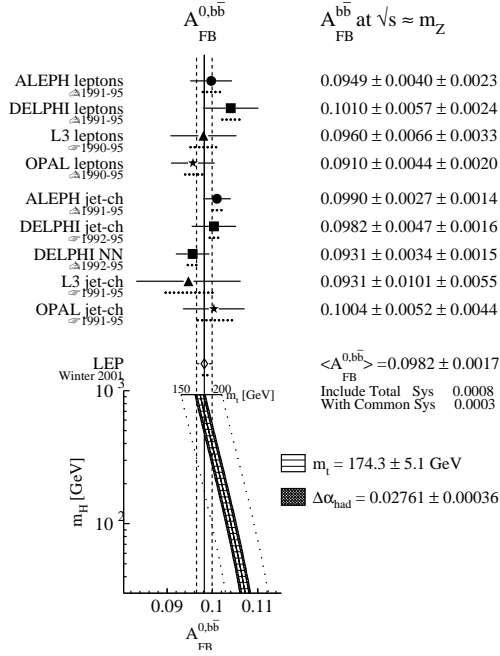


Figure 1: Measurements of  $A_{FB}^{0,b\bar{b}}$  at LEP. The lower plot shows the prediction of the Standard Model as a function of  $M_H$ . The width of the band is due to the uncertainties on  $\Delta\alpha_{had}^5$  and  $m_{top}$  added linearly.

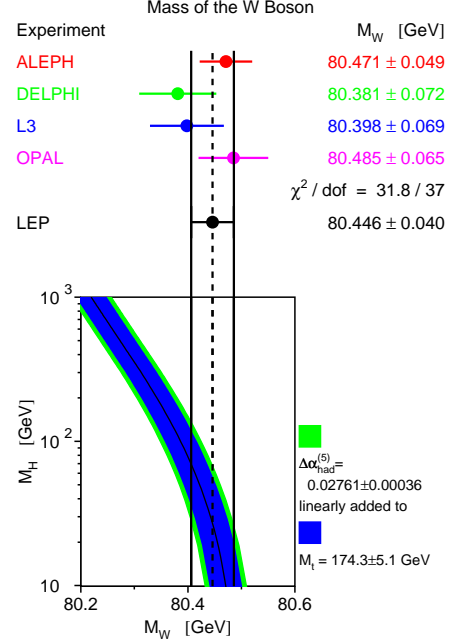


Figure 2: The measurement of  $M_W$  at LEP. The lower plot shows the prediction of the Standard Model as a function of  $M_H$ . The width of the band is due to the uncertainties on  $\Delta\alpha_{had}^5$  and  $m_{top}$  added linearly.

these improvements the systematic uncertainty has been reduced by a factor of 2 with respect to the old value<sup>10</sup>:

$$A_{FB}^{b\bar{b}}(\sqrt{s} \simeq M_Z) = 0.0990 \pm 0.0027 \pm 0.0014 \quad (2)$$

$$\text{old value : } A_{FB}^{b\bar{b}}(\sqrt{s} \simeq M_Z) = 0.1017 \pm 0.0038 \pm 0.0032 \quad (3)$$

Figure 1 shows all the  $A_{FB}^{b\bar{b}}$  measurements.

### The W mass

At LEP2 the W mass is determined<sup>5</sup> from the data recorded at centre-of-mass energies  $\sqrt{s} = 161 - 209$  GeV. Only ALEPH and L3 have analysed the year 2000 data and have an integrated luminosity of  $700 \text{ pb}^{-1}$  per experiment. The DELPHI and OPAL results are based on only  $450 \text{ pb}^{-1}$  per experiment.

Moreover ALEPH has done further systematic studies<sup>11</sup> leading to a significantly reduced uncertainty. The fragmentation uncertainty which is based on Monte Carlo comparisons is reduced from 30 MeV to 15 MeV. The uncertainty arising from final state interaction between the two W's (Bose Einstein Correlation and Color Reconnection) has also been re-estimated.

The LEP combined W mass obtained from the  $q\bar{q}l\bar{l}_1$  and  $q\bar{q}q\bar{q}$  channels are consistent:

$$\Delta M_W(q\bar{q}q\bar{q} - q\bar{q}l\bar{l}_1) = +18 \pm 46 \text{ MeV}$$

showing no evidence for a bias arising from FSI effects. The LEP W mass measurement is shown in Figure 2:

$$M_W = 80.446 \pm 0.026(\text{stat}) \pm 0.030(\text{syst}) \text{ GeV} \quad (4)$$

The combination with the CDF, D0 and UA2 measurements gives:

$$M_W = 80.448 \pm 0.034 \text{ GeV} \quad (5)$$

## $\alpha_{\text{QED}}(M_Z^2)$

As pointed out in section 1 the value of the QED coupling constant at  $\sqrt{s} = M_Z$ ,  $\alpha_{\text{QED}}(M_Z^2)$  is needed in the fits. The running of  $\alpha_{\text{QED}}$  is given by:

$$\alpha(s) = \frac{\alpha(0)}{1 - \Delta\alpha_l(s) - \Delta\alpha_{\text{had}}^5(s) - \Delta\alpha_{\text{top}}(s)} \quad (6)$$

$\Delta\alpha_l(s)$  and  $\Delta\alpha_{\text{top}}(s)$  are well known while  $\Delta\alpha_{\text{had}}^5(s)$  involves hadron loops at low energy and therefore non perturbative QCD. This can nevertheless be experimentally determined using the low energy  $e^+e^-$  data since  $\Delta\alpha_{\text{had}}^5(s)$  is related to  $R_{\text{had}} = \frac{\sigma(e^+e^- \rightarrow \text{hadrons})}{\sigma(e^+e^- \rightarrow \mu^+\mu^-)}$  via a dispersion integral.

In the previous determinations<sup>12</sup> of  $\Delta\alpha_{\text{had}}^5(s)$  the dominant error came from data taken in the range  $2 < \sqrt{s} < 5$  GeV. The error in this energy range has been reduced by a factor of more than 2 using new  $e^+e^-$  data from the BES experiment<sup>6</sup>.

A new determination of  $\Delta\alpha_{\text{had}}^5$  has been done<sup>7</sup> using only experimental data below 12 GeV and third order QCD above, leading to

$$\Delta\alpha_{\text{had}}^5(M_Z) = 0.02761 \pm 0.00036 \quad (7)$$

The error has been reduced by almost a factor 2 with respect to the previous value used in the electroweak fit<sup>12</sup>:  $\Delta\alpha_{\text{had}}^5(M_Z) = 0.02804 \pm 0.00065$ . Another determination including the BES data but more theoretical inputs in the low energy region<sup>13</sup>,  $\Delta\alpha_{\text{had}}^5(M_Z) = 0.02738 \pm 0.00020$ , will also be used in the fit for comparison.

### 2.3 Sensitivity to the Higgs mass

Figure 3 shows the sensitivity of some asymmetries and of the W mass to the Higgs mass. The experimental measurements are shown as well as the Standard Model prediction. The width of the Standard Model band shows the uncertainty arising from the precision on  $\Delta\alpha_{\text{had}}^5$ ,  $m_{\text{top}}$  and  $\alpha_s$ . The asymmetries are very sensitive to the Higgs mass. The W mass is also sensitive but it is very dependent on  $m_{\text{top}}$ .

All the asymmetry measurements can be converted into the measurement of the single parameter  $\sin^2\theta_{\text{eff}}^{\text{lept}}$  (Figure 4). The combination of these measurements gives

$$\sin^2\theta_{\text{eff}}^{\text{lept}} = 0.23156 \pm 0.00017 \quad (8)$$

The  $\chi^2$  of the fit is bad:  $\chi^2/d.o.f. = 15.5/6$ . This reflects the fact that the combined value of  $\sin^2\theta_{\text{eff}}^{\text{lept}}$  obtained from the leptonic asymmetries is  $3.6\sigma$  apart from that obtained with the quark asymmetries. This effect is mainly caused by the 2 most precise measurements,  $A_{\text{FB}}^{0,b\bar{b}}$  at LEP and  $A_l$  from SLD. Since the previous combination,  $A_{\text{FB}}^{0,b\bar{b}}$  has been more precisely measured as explained in section 2.2 and its value has slightly decreased, and so preferring a high Higgs mass (around 600 GeV). On the contrary the leptonic asymmetries prefer a light Higgs (around 60 GeV). This dispersion is interpreted here as a fluctuation in one or more of the measurements.

## 3 Test of the Standard Model

In the following the ZFITTER<sup>14</sup> and TOPAZ0<sup>15</sup> programs are used for all the fits. Using all the measurements discussed in section 2.1 except the direct measurement of  $M_W$  and  $m_{\text{top}}$  a fit to the Standard Model is performed to obtain an indirect determination of  $M_W$  and  $m_{\text{top}}$  and a

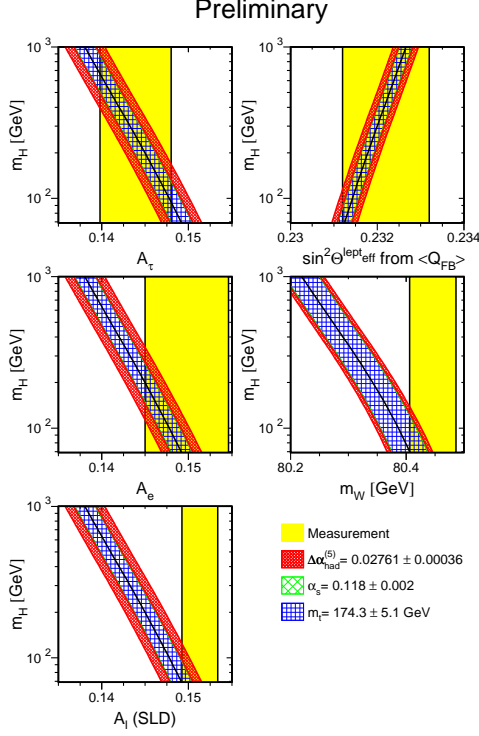


Figure 3: Sensitivity of some asymmetries and of  $M_W$  to the Higgs mass. The width of the Standard Model band gives the uncertainty arising from the precision on  $\Delta\alpha_{\text{had}}^5$  and  $m_{\text{top}}$  and  $\alpha_s$  added linearly.

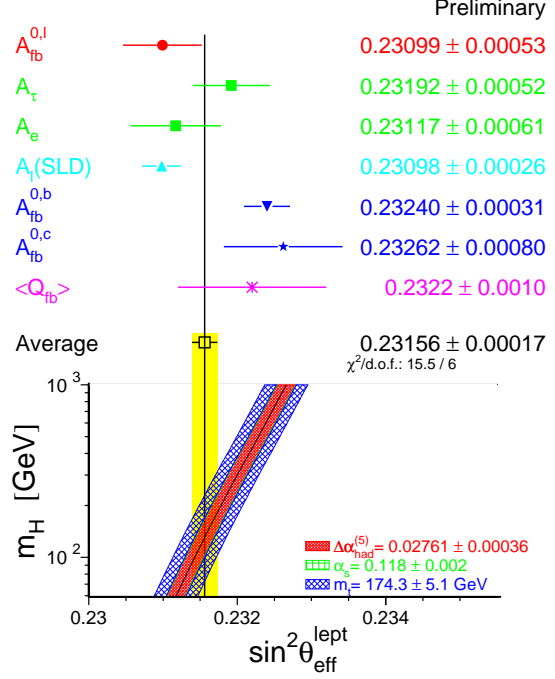


Figure 4: Determination of  $\sin^2\theta_{\text{eff}}^{\text{lept}}$  from the asymmetry measurements. The Standard Model prediction as a function of  $M_H$  is also shown. The width of this prediction gives the uncertainty arising from the band on  $\Delta\alpha_{\text{had}}^5$  and  $m_{\text{top}}$  and  $\alpha_s$  added linearly.

constraint on  $M_H$ . Figure 5 shows the result of that fit as well as the direct measurements (the 68% C.L. contours are shown). This indirect determination gives

$$m_{\text{top}} = 168.3_{-9.3}^{+11.9} \text{ GeV} \quad (9)$$

$$M_W = 80.357 \pm 0.033 \text{ GeV} \quad (10)$$

$$\text{Log}(M_H) = 1.94_{-0.30}^{+0.37} \quad (11)$$

$$M_H = 87_{-43}^{+119} \text{ GeV} \quad (12)$$

in agreement with the direct measurements:

$$m_{\text{top}} = 174.3 \pm 5.1 \text{ GeV} \quad (13)$$

$$M_W = 80.448 \pm 0.034 \text{ GeV} \quad (14)$$

The Standard Model prediction is also shown in Figure 5 showing that a low Higgs mass is preferred by both the direct and indirect  $M_W$  and  $m_{\text{top}}$  values.

## 4 Constraint on the Higgs mass

### 4.1 The global fit

The agreement between the direct and the indirect determination of  $M_W$  and  $m_{\text{top}}$  (section 3) shows the consistency of the Standard Model. These direct measurements are then used to obtain a better constraint on the Higgs mass. Using the new value of  $\Delta\alpha_{\text{had}}^5$  discussed in section 2.2 the result of the fit is:

$$\text{Log}(M_H) = 1.99 \pm 0.21 \quad (15)$$

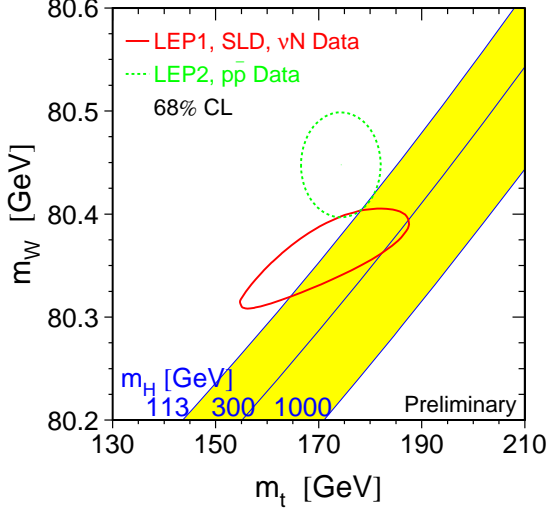


Figure 5: Indirect determination of  $m_{\text{top}}$  and  $M_W$  (full line) compared to the direct measurements (dotted line). The 68% C.L. contours are shown. The band shows the Standard Model prediction for a Higgs mass ranging from 113 GeV to 1 TeV.

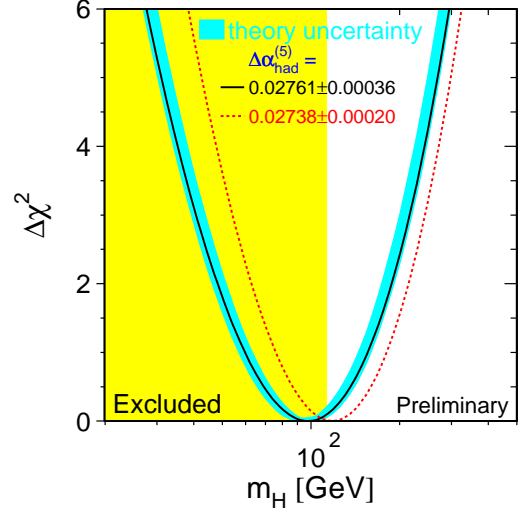


Figure 6:  $\Delta\chi^2 = \chi^2 - \chi_{\text{min}}^2$  as a function of  $M_H$  for the global fit to the Standard Model. The region excluded by the direct searches at LEP is also shown.

$$M_H = 98_{-38}^{+58} \text{ GeV} \quad (16)$$

$$m_{\text{top}} = 175.7 \pm 4.4 \text{ GeV} \quad (17)$$

$$M_W = 80.393 \pm 0.019 \text{ GeV} \quad (18)$$

leading to an upper limit on the Higgs mass:  $M_H < 212$  GeV at 95% C.L. Again the  $\chi^2$  is bad,  $\chi^2/d.o.f. = 25/15$  which corresponds to a probability of only 4%. This is simply a reflection of the the disagreement between the asymmetry measurements already discussed in section 2.3. Figure 6 shows the  $\Delta\chi^2 = \chi^2 - \chi_{\text{min}}^2$  as a function of the Higgs mass. The dotted line shows the result of the fit using a more theory driven determination of  $\Delta\alpha_{\text{had}}^5$ <sup>13</sup> which also includes the new BES data.

The new value of  $\Delta\alpha_{\text{had}}^5$  results in a shift of the preferred Higgs mass of about +35 GeV and a significant reduction in the error: the error on  $\text{Log}(M_H)$  arising from  $\Delta\alpha_{\text{had}}^5$  has decreased from 0.2 to 0.1. This is no longer the single dominant error, but still one of the limiting errors.

#### 4.2 The uncertainty on $M_H$

In order to determine which measurements need to be improved to better constrain the Higgs mass the error on  $\text{Log}(M_H)$  can be broken down into the different sources. For this purpose only the two most powerful variables,  $\sin^2\theta_{\text{eff}}^{\text{lept}}$  and  $M_W$ , are used separately. The parametrisation of the  $\sin^2\theta_{\text{eff}}^{\text{lept}}$  and  $M_W$  dependance with  $m_{\text{top}}^2$ ,  $\text{Log}(M_H)$  and  $\Delta\alpha_{\text{had}}^5$  given in Ref.<sup>16</sup> is used to propagate the experimental errors. Using  $\sin^2\theta_{\text{eff}}^{\text{lept}}$  alone the uncertainty on  $\text{Log}(M_H)$  is

$$\delta\text{Log}(M_H) = \pm 0.14(\delta\sin^2\theta_{\text{lept}}^{\text{eff}}) \mp 0.10(\delta\Delta\alpha_{\text{had}}^5) \pm 0.13(\delta m_{\text{top}}) = \pm 0.22 \quad (19)$$

and using  $M_W$  alone:

$$\delta\text{Log}(M_H) = \mp 0.24(\delta M_W) \mp 0.05(\delta\Delta\alpha_{\text{had}}^5) \pm 0.26(\delta m_{\text{top}}) = \pm 0.36 \quad (20)$$

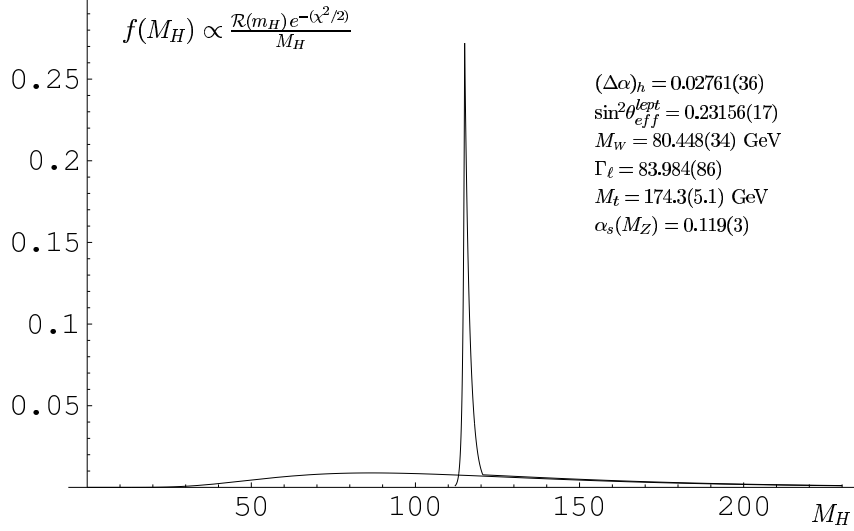


Figure 7: Probability density function  $f(M_H)$ . The lower curve shows the indirect measurements alone and the curve with the spike at  $\sim 115$  GeV shows the combination with the direct search.

The error arising from  $\Delta\alpha_{\text{had}}^5$  is no more the dominant one and with the present uncertainty on  $M_W$  and on  $m_{\text{top}}$   $\sin^2\theta_{\text{eff}}^{\text{lept}}$  is more powerful than  $M_W$ . The large dependence of  $M_W$  on  $m_{\text{top}}$  limits the power of  $M_W$  in constraining  $M_H$ . Therefore one also needs to improve the precision of  $m_{\text{top}}$  in order to increase the power of  $M_W$ . Assuming that at the end of Run IIa of the Tevatron<sup>17</sup> the error on  $m_{\text{top}}$  is reduced to 2.5 GeV and on  $M_W$  to 25 MeV (LEP 2 and Tevatron combined) then one would get using  $\sin^2\theta_{\text{eff}}^{\text{lept}}$  alone:

$$\delta\text{Log}(M_H) = \pm 0.14(\delta\sin^2\theta_{\text{lept}}^{\text{eff}}) \mp 0.10(\delta\Delta\alpha_{\text{had}}^5) \pm 0.07(\delta m_{\text{top}}) = \pm 0.19 \quad (21)$$

and using  $M_W$  alone:

$$\delta\text{Log}(M_H) = \mp 0.14(\delta M_W) \mp 0.05(\delta\Delta\alpha_{\text{had}}^5) \pm 0.12(\delta m_{\text{top}}) = \pm 0.19 \quad (22)$$

$M_W$  would then be as powerful as  $\sin^2\theta_{\text{eff}}^{\text{lept}}$  for constraining  $M_H$ . Note that these numbers are obtained assuming that the value of  $M_H$  is of the order of 100 GeV.

#### 4.3 Combination with the direct search

In Figure 6 the lower limit on the Higgs mass obtained from the direct searches at LEP2 is also shown, but this information is not used in the fit. The likelihood  $\mathcal{R}(M_H)$  obtained from the direct searches<sup>18</sup> is combined with the  $\chi^2$  probability obtained from the indirect measurements in Ref.<sup>19</sup>.  $\mathcal{R}(M_H)$  includes the information from the excess of events observed in the year 2000 at a mass around 115 GeV. This combination uses a Bayesian approach, assuming a uniform prior in  $\text{Log}(M_H)$ . The probability density function  $f(M_H) \propto \frac{\mathcal{R}(M_H)e^{(-x^2/2)}}{M_H}$  is shown in Figure 7. The spike at  $M_H \simeq 115$  GeV is due to the excess of events in the direct search. The effect of this excess is to concentrate most of the probability around 115 GeV. About 50% of the probability is contained between a mass of 113 GeV and 120 GeV. Note also that the 95% upper limit goes up by about 20 GeV when the direct search is taken into account.

## 5 Conclusion

LEP1 and SLD results are final except the heavy flavour results. The values of  $\sin^2\theta_{\text{eff}}^{\text{lept}}$  extracted from the leptonic asymmetries and from the quark asymmetries are  $3.6\sigma$  apart. This effect is

interpreted here as a fluctuation in one or more of the measurements.

The new BES data lead to a significant improvement in the determination of  $\Delta\alpha_{\text{had}}^5$  which used to be the dominant source of error in the electroweak fit.

The full LEP2 data set is not yet analysed for the W mass measurement. Moreover systematic uncertainties should be reduced with studies of the full data set.

Thanks to the statistics which will be accumulated during RunIIa at the Tevatron the uncertainty on the top mass and on the W mass will be significantly reduced allowing us to make more precise tests of the Standard Model and to constrain better the Higgs mass.

## Acknowledgments

I would like to thank the LEP Electroweak Working group for providing me with the results and the plots. I also thank G. Degrassi for kindly sending me his results.

## References

1. The LEP Collaborations and the Line Shape Sub-group of the LEP Electroweak Working Group *CERN-EP-2000-153*, to appear in *Phys. Rep.*
2. The ALEPH Collaboration, Measurement of  $A_{\text{FB}}^{\text{bb}}$  using Inclusive b-hadron Decays, *ALEPH-CONF/2001-020*.
3. The DELPHI Collaboration, Determination of  $A_{\text{FB}}^{\text{bb}}$  using inclusive charge reconstruction and lifetime tagging at LEP 1, *DELPHI/2001-027 CONF 468*.
4. N. de Groot, in these proceedings.
5. The LEP Collaborations and the LEPEW Working Group, *LEPEWWG/MASS/2000-01*.
6. The BES Collaboration, J.Z. Bai *et al*, hep-ex/01023003 and G. Huang, contribution to these proceedings.
7. H. Burkhardt and B. Pietrzyk, LAPP-EXP 2001-03, accepted by *Phys. Lett. B*.
8. The LEP Collaborations, the LEP Electroweak Working Group and the SLD Heavy Flavour and Electroweak Groups, *CERN-EP/2001-021*.
9. The LEP Electroweak Working Group: <http://lepewwg.web.cern.ch/LEPEWWG/>
10. The ALEPH Collaboration, Determination of  $A_{\text{FB}}^{\text{bb}}$  using Jet Charge Measurements in Z Decays, *Phys. Lett. B* **426**, 217 (1998).
11. The ALEPH Collaboration, Measurement of the W Mass and Width in  $e^+e^-$  Collisions at  $\sqrt{s}$  between 192 and 208 GeV, *ALEPH-CONF/2001-017*.
12. S. Eidelmann and F. Jegerlehner, *Z. Phys. C* **67**, 585 (1995).
13. A. Martin, J. Outwaite and M.G. Ryskin, *Phys. Lett. B* **492**, 69 (2000).
14. D. Bardin *et al.*, *Z. Phys. C* **44**, 493 (1989); *C.P.C* **59**, 303 (1990); ZFITTER v.6.21:DESY 99-070(1999), hep-ph/9908433 to appear in *Comp. Phys. Comm.* .
15. G. Montagna *et al.*, *Comp. Phys. Comm.* **117**, 278 (1999).
16. G. Degrassi, P. Gambino, *Nucl. Phys. B* **567**, 3 (2000).
17. D. Glensinski, contribution to these proceedings.
18. P. Igo-Kemenes, Talk given at the LEPC of November 3, 2000.
19. G. Degrassi, Talk presented at 50 Years of Electroweak Physics, New York, 27-28 Oct 2000 hep-ph/0102137.